

## Anomalous behavior of the magnetic entropy in PrNi<sub>5</sub>

P. J. von Ranke\*

*Ames Laboratory, Iowa State University, Ames, Iowa 50011-3020*

V. K. Pecharsky and K. A. Gschneidner, Jr.

*Ames Laboratory, Iowa State University, Ames, Iowa 50011-3020*

*and Department of Materials Science and Engineering, Iowa State University, Ames, Iowa 50011-3110*

B. J. Korte<sup>†</sup>

*Ames Laboratory, Iowa State University, Ames, Iowa 50011-3020*

(Received 16 June 1998)

By considering a Hamiltonian that includes the crystalline electric field and exchange interaction components we showed theoretically that paramagnetic PrNi<sub>5</sub> exhibits an anomalous entropy behavior in which the magnetic entropy increases with increasing magnetic field at low temperature. This anomaly in magnetic entropy can be fully understood and is associated with the crossing of the two lowest magnetic energy levels ( $\Gamma_4$  and  $\Gamma_1$ ). Experimental verification of the anomalous behavior of the magnetic entropy in polycrystalline PrNi<sub>5</sub> was obtained. [S0163-1829(98)02045-1]

### INTRODUCTION

The magnetic properties of paramagnetic PrNi<sub>5</sub> have been extensively studied because this material is used as a working medium to reach the ultralow temperature of about 1 mK by the nuclear adiabatic demagnetization technique.<sup>1</sup> The possibility of application of the reversible magnetization-demagnetization for cooling (and also heating) near room temperature<sup>2</sup> has recently received much attention,<sup>3,4</sup> and an understanding of the magnetocaloric properties of lanthanide intermetallics takes on a fundamental importance.

The compound PrNi<sub>5</sub> crystallizes in the hexagonal CaCu<sub>5</sub>-type structure<sup>5</sup> and its magnetism is due to the Pr<sup>3+</sup> ions in PrNi<sub>5</sub>. Therefore, the simplest theoretical approximation to model the magnetic properties of PrNi<sub>5</sub> is to consider a Hamiltonian which includes the crystalline electric field (CEF) in hexagonal symmetry and the exchange interactions. The CEF can be treated by using the so-called point-charge model<sup>6</sup> and the exchange interaction by using a molecular field approximation.

The theoretical magnetization and magnetic entropy of PrNi<sub>5</sub> were investigated for single crystalline and polycrystalline specimens using the models mentioned in the previous paragraph. Theoretical calculations of the thermal and magnetic properties of polycrystalline specimens were made by taking the average values of the magnetization and magnetic entropy, which were determined for a single crystal along the three main crystallographic directions, i.e., along the  $a[10\bar{1}0]$ ,  $b[01\bar{1}0]$ , and  $c[0001]$  axes of the hexagonal unit cell.

The theoretical calculations were carried out using a value of the molecular field exchange parameter estimated to be equal to  $\lambda = 0.1 \text{ meV} = 29.84T^2/\text{meV}$ ,<sup>7,8</sup> and several different sets of CEF parameters reported for PrNi<sub>5</sub>.<sup>9-12</sup> For all sets of CEF parameters we observe a crossing of the two lowest CEF energy levels ( $\Gamma_4$  and  $\Gamma_1$ ) when the external magnetic field applied along the easy axis reaches a certain

critical value. These crossings are clearly observed as a jump in the magnetization at low temperature ( $T \sim 0.3 \text{ K}$ ), in the magnetization versus magnetic field curves. In this paper we present an explanation of the origin of the theoretically predicted anomaly in the magnetic entropy of PrNi<sub>5</sub> and a comparison of the theory with experiment.

### THEORY

The magnetism in the intermetallic compound PrNi<sub>5</sub> is due only to the Pr<sup>3+</sup> ions since the Ni ions in this alloy are nonmagnetic. Thus, magnetic properties of PrNi<sub>5</sub> can be described by a Hamiltonian that takes into account the CEF and exchange interactions given by

$$\hat{H} = \hat{H}_{\text{CEF}} + \hat{H}_{\text{mag}}, \quad (1)$$

where

$$\hat{H}_{\text{CEF}} = B_2^0 O_2^0 + B_4^0 O_4^0 + B_6^0 O_6^0 + B_6^6 O_6^6 \quad (2)$$

and

$$\hat{H}_{\text{mag}} = -g \mu_B H_m J^z, \quad (3)$$

where

$$H_m = H_0 + \lambda M. \quad (4)$$

Relation (2) is the single ion CEF Hamiltonian for the hexagonal symmetry, where  $O_n^m$  are Stevens' equivalent operators,<sup>13</sup> and the four constants  $B_n^m$  determine the CEF potential. For PrNi<sub>5</sub> these constants were determined most reliably from inelastic neutron scattering measurements<sup>9</sup> and have the following values:  $B_2^0 = 0.61$ ,  $B_4^0 = 0.00496$ ,  $B_6^0 = 0.000101$ , and  $B_6^6 = 0.0027$  (in meV). Using these CEF parameters in relation (2), the ninefold degenerate ground multiplet  ${}^3H_4$  of Pr<sup>3+</sup> is split into the following crystal-field level scheme: singlet  $\Gamma_4(0)$ , singlet  $\Gamma_1(1.50 \text{ meV})$ , doublet

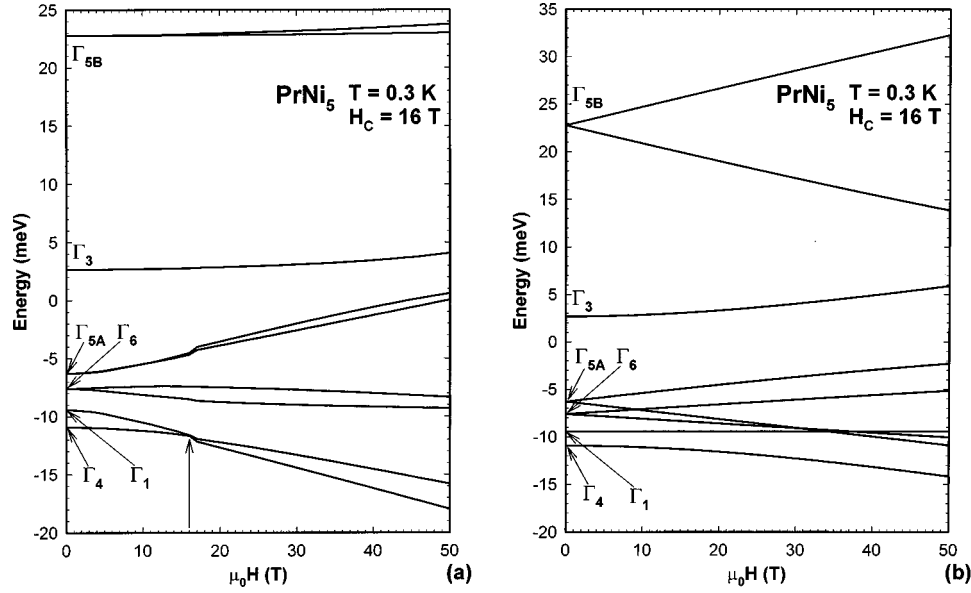


FIG. 1. (a) Magnetic energy levels in PrNi<sub>5</sub> for a magnetic field applied along the *a* axis, calculated at  $T=0.3$  K, using the exchange parameter  $\lambda = 29.84$  T<sup>2</sup>/meV and the CEF values from Ref. 9. (b) Magnetic energy levels in PrNi<sub>5</sub> for a magnetic field applied along the *c* axis, calculated at  $T=0.3$  K, using the exchange parameter  $\lambda = 29.84$  T<sup>2</sup>/meV and the CEF values from Ref. 9. The arrow in (a) indicates the critical field  $H_c = 16$  T for the crossing of the two lowest levels.

$\Gamma_6$  (3.35 meV), doublet  $\Gamma_{5A}$  (4.65 meV), singlet  $\Gamma_3$  (13.6 meV), and doublet  $\Gamma_{5B}$  (33.71 meV) see Figs. 1(a) and 1(b).

Relation (3) is the single ion magnetic Hamiltonian, taken in the molecular field approximation, where  $g$  is the Lande factor,  $\mu_B$  is the Bohr magneton, and  $H_m$  is the exchange field given by relation (4) where,  $H_0$  is the external magnetic field,  $\lambda$  is the molecular field constant, and  $M$  is the magnetization.

The magnetic state equation is obtained taking the Boltzmann mean value of the magnetic dipole operator:

$$M = g \mu_B \langle J^\eta \rangle = g \mu_B \frac{\sum \langle \varepsilon_i | J^\eta | \varepsilon_i \rangle \exp(-\varepsilon_i / KT)}{\sum \exp(-\varepsilon_i / KT)}. \quad (5)$$

In Eq. (5)  $\varepsilon_i$  and  $|\varepsilon_i\rangle$  are, respectively, the energy eigenvalues and eigenvectors of Hamiltonian (1) and  $J^\eta$  is the component of the total angular momentum in an arbitrary direction  $\eta$ . For PrNi<sub>5</sub> the easy magnetic direction is the  $a[10\bar{1}0]$  crystallographic direction; in this way  $\eta = a = x$  since we have adopted the *c* crystallographic direction as the quantization direction (i.e.,  $\eta = z$  for *c* direction). The magnetization is determined by self-consistently solving Eqs. (4) and (5).

In order to extend the above procedure for the calculation of the magnetization of polycrystalline specimens, it is necessary to take into account the magnetization along the three main crystallographic directions (i.e., along the *a*, *b*, and *c* axes) of the hexagonal unit cell which is equal to

$$M = \frac{g \mu_B}{3} (\langle J^a \rangle + \langle J^b \rangle + \langle J^c \rangle) = \frac{g \mu_B}{3} (2 \langle J^x \rangle + \langle J^z \rangle). \quad (6)$$

In a hexagonal lattice  $\langle J^a \rangle = \langle J^b \rangle$ . Therefore, the theoretical magnetization calculation for the PrNi<sub>5</sub> single crystal is determined by self-consistently solving Eqs. (4) and (5) (with  $\eta = x$ ), and for polycrystalline PrNi<sub>5</sub> we must use Eq.

(6) in the place of Eq. (5). The molar magnetic contribution to the entropy is obtained using the relation

$$S_{\text{mag}} = R \left[ \ln \left( \sum \exp \left( -\frac{\varepsilon_i}{KT} \right) \right) + \frac{\langle E \rangle}{KT} \right], \quad (7)$$

where  $\langle E \rangle$  is the mean energy and  $R$  is the universal gas constant.

In order to perform theoretical calculations of the temperature and magnetic field dependence of the entropy in polycrystalline PrNi<sub>5</sub>, we again considered an average of the values with magnetic field applied parallel to the three crystallographic directions, and this gives the following expression:

$$S_{\text{mag}}(H) = \frac{2S_a(H) + S_c(H)}{3}, \quad (8)$$

where  $S_a(H)$  and  $S_c(H)$  are magnetic entropies as functions of field applied along *a* and *c* crystallographic directions. It should be noted that relation (8) must be applied under the condition of a self-consistent solution of Eqs. (4) and (6).

## RESULTS FOR PrNi<sub>5</sub>

Using the four CEF parameters cited above and the exchange parameter  $\lambda = 29.84$  T<sup>2</sup>/meV for PrNi<sub>5</sub> and solving

TABLE I. Crystalline electric field parameters of PrNi<sub>5</sub> (in meV) and the critical crossing field in T.

Reference	$B_2^0$	$B_4^0 \times 10^2$	$B_6^0 \times 10^4$	$B_6^6 \times 10^2$	$H_c$
9	0.61	0.496	1.01	0.27	16
10	0.48	0.362	0.81	0.26	18
11	0.50	0.389	0.76	0.27	21.3
12	0.50	0.448	0.69	0.267	34

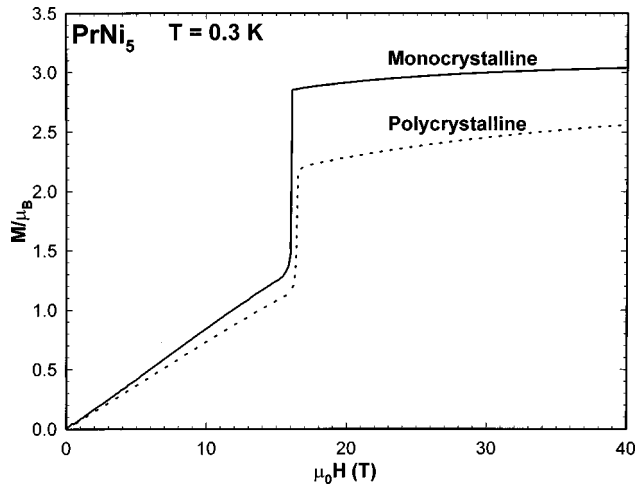


FIG. 2. The magnetization vs magnetic field applied along the  $a$  axis for  $\text{PrNi}_5$  calculated at  $T=0.3$  K, using the exchange parameter  $\lambda = 29.84 T^2/\text{meV}$  and the CEF values from Ref. 9. The solid and dotted lines represent the theoretical results for monocrystalline and polycrystalline samples, respectively.

Eq. (1), we have plotted the energy eigenvalues versus magnetic field at  $T=0.3$  K for both  $a$  and  $c$  directions [Figs. 1(a) and 1(b), respectively]. We note that in Fig. 1(a), the crossing of the two lowest levels occurs at a critical magnetic field  $H_c \cong 16$  T. The effect of this crossing is of fundamental importance for understanding the anomalous behavior of the magnetic entropy and will be discussed later in this paper. Table I shows other CEF parameters found in the literature with the corresponding critical magnetic field  $H_c$ , determined using the same exchange parameter ( $\lambda = 29.84T^2/\text{meV}$ ) and  $T=0.3$  K.

The results of our theoretical calculations at  $T=0.3$  K for the magnetization as a function of magnetic field are displayed in Fig. 2. The jump in the magnetization at  $H=H_c \cong 16$  T is expected to be observed at low temperature, since

the magnetic moment reflects the derivative of the energy levels with respect to the exchange field  $\langle \varepsilon_i | J^\eta | \varepsilon_i \rangle \sim \partial \varepsilon_i / \partial H_m$ .

Figures 3(a) and 3(b) show the theoretical results for the temperature dependence of the magnetic entropy of monocrystalline and polycrystalline  $\text{PrNi}_5$ , respectively, in magnetic fields of 0, 7, 16, and 20 T. In both Fig. 3(a) and 3(b), we note that (1) for  $T \geq 14$  K, the entropy decreases with increasing magnetic field (the typical behavior for a paramagnet) and (2) for  $T \leq 11$  K the magnetic entropy below the critical field ( $H_c = 16$  T) shows the opposite behavior, i.e., the magnetic entropy increases with increasing magnetic field, which is anomalous. The inset to Fig. 3(a) shows that the crossing of the CEF levels at  $H=16$  T and  $T=0.3$  K gives rise to a peak in the magnetic entropy.

Figure 4 shows the theoretical curves for the temperature dependence of the isothermal magnetic entropy change  $-\Delta S_{\text{mag}}$  as the magnetic field changes from 0 to 7 T. As expected from Figs. 3(a) and 3(b), below  $\sim 14$  K, the  $-\Delta S_{\text{mag}}$  is negative for both polycrystalline and monocrystalline  $\text{PrNi}_5$  samples. It is worth noting that the anomalous negative  $-\Delta S_{\text{mag}}$  is more pronounced in monocrystalline compound when magnetic field is applied along the easy magnetic axis.

Figure 5 shows the theoretical  $-\Delta S_{\text{mag}}$  versus temperature in polycrystalline  $\text{PrNi}_5$  samples calculated using different sets of CEF parameters given in Table I. These curves were also calculated for a magnetic field change from 0 to 7 T using the same exchange parameter ( $\lambda = 29.84T^2/\text{meV}$ ). It is easy to see that regardless of the choice of CEF parameters the  $-\Delta S_{\text{mag}}$  features a low-temperature minimum and a high-temperature maximum. However, the different sets of CEF parameters result in different temperatures and entropy values at both the maximum and minimum.

## EXPERIMENT

In order to verify the theoretical prediction of the anomalous behavior of the magnetic entropy in  $\text{PrNi}_5$  we prepared

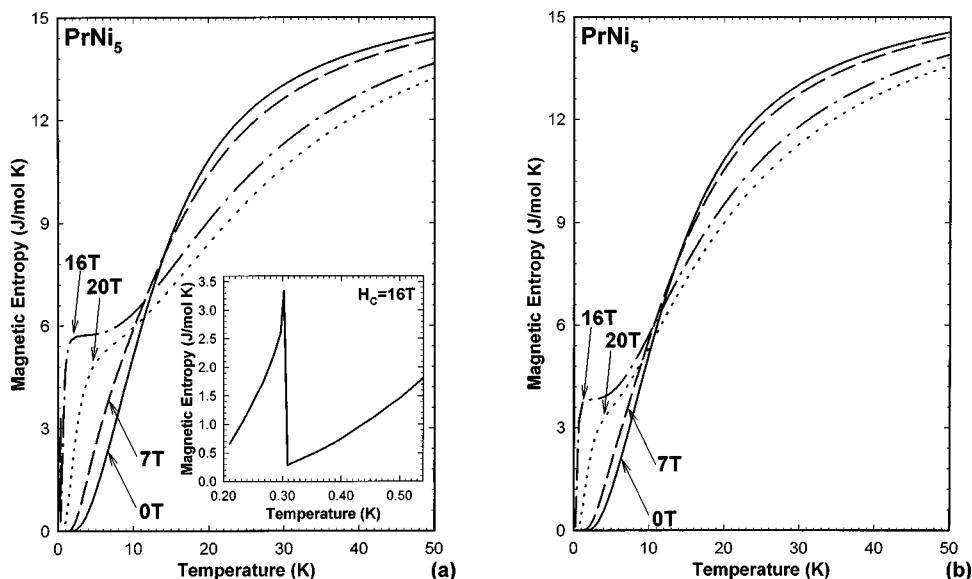


FIG. 3. (a) Theoretical magnetic entropy vs temperature in monocrystalline  $\text{PrNi}_5$  for different magnetic fields applied along the  $a$  axis. The crossing of the CEF levels at  $H_c = 16$  T at  $T=0.3$  K gives rise to a peak in entropy as shown in the inset. (b) Theoretical magnetic entropy vs temperature in polycrystalline  $\text{PrNi}_5$  for different magnetic fields.

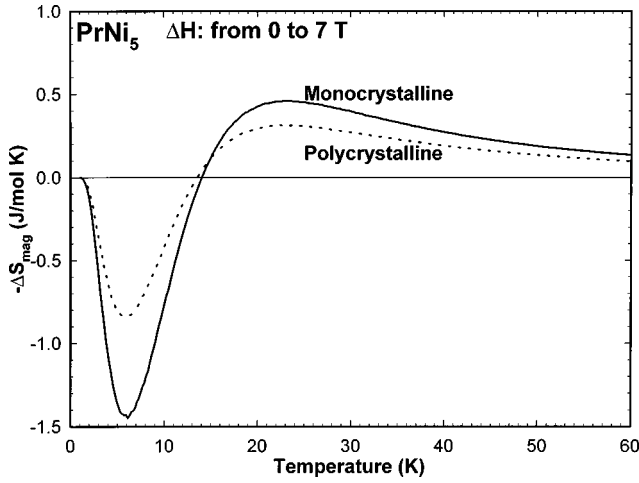


FIG. 4. Theoretical temperature dependence of the isothermal  $-\Delta S_{\text{mag}}$  in  $\text{PrNi}_5$ , using the exchange parameter  $\lambda = 29.84 T^2/\text{meV}$  and the CEF values from Ref. 9. Solid and dotted lines represent the monocrystalline and polycrystalline samples, respectively, for a magnetic field change from 0 to 7 T. The data for single crystal are shown for magnetic field parallel to the  $a$  axis.

a polycrystalline sample and measured its heat capacity in 0 and 7 T magnetic fields. The sample was arc melted from pure constituents in an argon atmosphere on water-cooled copper hearth. The Pr was prepared by the Materials Preparation Center, Ames Laboratory and was 99.89 at. % (99.99 wt. %) pure with major impurities (in ppm atomic) as follows: H-697, N-151, O-79, C-47, Ta-29, F-22, Cl-10, Si-10, and Fe-10. The Ni was purchased commercially and was 99.99 wt. % pure. The alloy (total weight approximately 18 g) was melted seven times with the button turned over after each melting to ensure the sample's homogeneity. The weight losses after arc melting were less than 0.25% and, therefore, the sample's composition was assumed to be unchanged. The x-ray powder diffraction analysis revealed that within the limits of detection (usually less than 5% of an

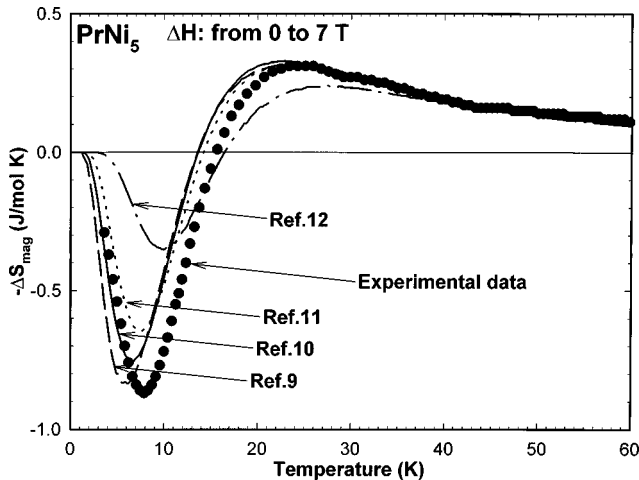


FIG. 5. Theoretical temperature dependence of the isothermal  $-\Delta S_{\text{mag}}$  in polycrystalline  $\text{PrNi}_5$  for a magnetic field changes from 0 to 7 T. These curves were calculated using  $\lambda = 29.84 T^2/\text{meV}$  and four different sets of CEF parameters. The experimental data calculated from heat capacity measured in 0 and 7 T magnetic fields are also shown as solid circles.

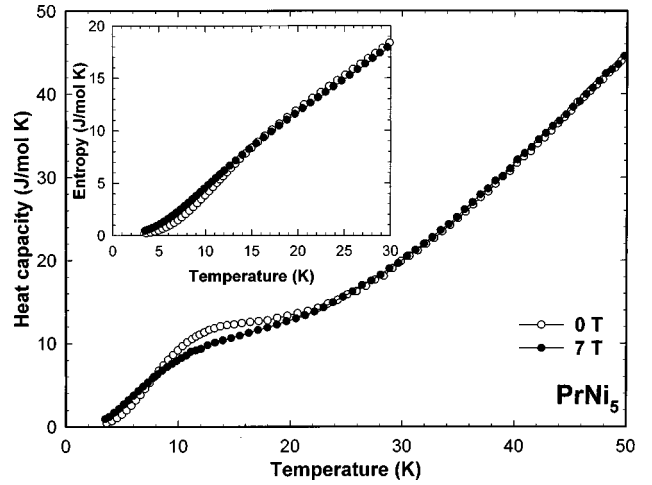


FIG. 6. The heat capacity of polycrystalline  $\text{PrNi}_5$  in 0 T (open circles) and 7 T (solid circles) magnetic fields from 3.4 to 50 K. The inset shows the total entropy in the same fields from 3.4 to 30 K.

impurity phase) the arc-melted alloy was single-phase material and, therefore, no heat treatment was performed.

The heat capacity was measured in an adiabatic heat-pulse calorimeter<sup>14</sup> from 3.4 to 350 K in 0 and 7 T magnetic fields. The total entropy was calculated from experimental heat capacity as

$$S(H) = \int_{3.4}^T \frac{C(H)}{T} dT, \quad (9)$$

where the lower limit of integration was common lowest temperature for 0 and 7 T sets of experimental data. The isothermal entropy change  $\Delta S_{\text{mag}}$  was then evaluated as the isothermal difference between  $S(0)$  and  $S(7)$ . The accuracy of experimental heat capacity and total entropy in the temperature range between 3.4 and 50 K was between 0.3 and 0.8 %.

The heat capacity of  $\text{PrNi}_5$  from 3.4 to 50 K is shown in Fig. 6 and the inset shows the behavior of the total entropy from 3.4 to 30 K, both in 0 and 7 T magnetic field. A broad heat capacity maximum observed between 12 and 16 K in the zero field data is a Schottky anomaly due to the low lying CEF energy levels. As seen, this maximum is suppressed by a 7 T magnetic field with the magnetic entropy shifted towards lower temperature. A direct comparison between the data shown in Fig. 3(b) and the inset in Fig. 6 is impossible because the experimental entropy is a sum of electronic, lattice, and magnetic entropies. Nonetheless, both calculated [Fig. 3(b)] and experimental (inset in Fig. 6) entropy in 7 T exceeds that in 0 T below  $\sim 15$  K (which is anomalous for a normal paramagnet), and above  $\sim 15$  K the 0 T entropy exceeds that of the 7 T. When one calculates the isothermal entropy change from these experimentally determined entropy functions, there is an excellent match with the behavior predicted theoretically; see Fig. 5. It is obvious that the best agreement is observed between the experimental results and the theoretical values using the CEF parameters from Ref. 9, although the  $\Delta S_{\text{mag}}$  values calculated using the CEF parameters given by Ref. 10 are also in fair agreement with experiment.

## DISCUSSION

The physical nature of the above described entropy vs temperature behavior in PrNi<sub>5</sub> can be readily understood in terms of magnetic field dependence of the two lowest CEF energy levels [see Fig. 1(a)]. When the magnetic field increases from zero to  $H_c = 16$  T the energy difference of these two levels goes to zero, and there is an increase of the density of states. Therefore, the magnetic entropy in low temperature region, where the Boltzmann population of these two lowest levels are dominant, must increase. On the other hand, when the magnetic field increases above the critical field,  $H_c = 16$  T, the energy difference of the two lowest levels begin to increase, and accordingly, the density of states decreases, and therefore, the entropy at 20 T becomes lower than that at 16 T in the entire temperature range [see the curves for  $H = 16$  and 20 T in Figs. 3(a) and 3(b)].

The inset of Fig. 3(a) shows a peak in magnetic entropy vs temperature at  $T \sim 0.3$  K and  $H_c \sim 16$  T. The appearance of this peak directly reflects the crossing of the two lowest levels. The thermodynamic coordinates ( $H_c \sim 16$  T and  $T \sim 0.3$  K) are the same where the crossing between the two lowest levels occurs in Fig. 1(a) (the point of a high density of states or large entropy). Fixing  $H = H_c \sim 16$  T, and increasing (or decreasing) the temperature from the value of  $T = 0.3$  K, the magnetization will decrease (or increase), and in both cases the density of states will decrease and so will the magnetic entropy.

Since the magnetic field dependence along the  $c$  axis does not exhibit a crossing of the two lowest CEF levels [see Fig. 1(b)] the entropy change  $-\Delta S_{\text{mag}}$  vs  $T$  is more pronounced in the case of monocrystalline sample than in the case of polycrystalline sample, as shown in Fig. 4.

Using different sets of CEF parameters given in Table I in our theoretical calculations for  $-\Delta S_{\text{mag}}$  vs  $T$  (for both monocrystalline and polycrystalline materials), we have observed that in all cases the crossing of the two lowest magnetic energy levels ( $\Gamma_4$  and  $\Gamma_1$ ) will always occur. Hence, the negative sign for  $-\Delta S_{\text{mag}}$  vs  $T$  is theoretically expected for PrNi<sub>5</sub>, at low temperature. Figure 5 shows the theoretical values of  $-\Delta S_{\text{mag}}$  vs  $T$  in polycrystalline PrNi<sub>5</sub> using the different sets of CEF parameters. As the  $H_c$  increases, the negative sign in the  $-\Delta S_{\text{mag}}$  vs  $T$  curve becomes less pronounced. As already mentioned above, the results of experimental measurements of  $\Delta S_{\text{mag}}$  for the magnetic field change from 0 to 7 T agree well with theoretically predicted values (Fig. 5). As expected, the CEF parameters determined from inelastic neutron scattering (Ref. 9) seems to be the most reliable because they show the best agreement between the theory and the experiment. Some differences could be ex-

plained by the assumption that the  $\Delta S_{\text{mag}}$  in polycrystalline material is just an average along the three major crystallographic directions [Eq. (8)]. Indeed, better agreement would be expected if the averaging was done along all possible crystallographic directions.

At  $T = 50$  K in a zero magnetic field the magnetic entropy for monocrystalline and polycrystalline PrNi<sub>5</sub> is approximately equal to 14.5 J/mol K which corresponds to  $\sim 80\%$  of the maximum theoretical magnetic entropy  $S_{\text{mag}}^{\text{max}} \sim 8.31 \ln(2J + 1) = 18.3$  J/mol K. At  $T = 50$  K in a magnetic field of 20 T the entropies are 13.2 and 13.6 J/mol K for the monocrystalline and polycrystalline specimens, respectively.

The theoretically calculated magnetic field dependence of magnetization (Fig. 2) shows jumps in the magnetization at a critical magnetic field  $H_c \sim 16$  T for the monocrystalline sample and  $H_c \sim 16.5$  T for the polycrystalline sample. The jumps in magnetization vs  $H$  curves smear out when the temperature increases and this has been theoretically studied elsewhere.<sup>8</sup>

## CONCLUSION

The magnetic entropy changes in paramagnetic PrNi<sub>5</sub> were theoretically investigated using a Hamiltonian which takes into account the crystalline electric field and exchange interaction. An anomalous increase of magnetic entropy was predicted to occur in applied magnetic fields at low temperatures. This behavior is unusual in a paramagnetic system since normally the effect of magnetic field on paramagnetic system is to align the magnetic moments parallel with the field direction, and therefore, to reduce the magnetic entropy. This anomaly is a direct consequence of the crossing of crystalline electric field levels ( $\Gamma_4$  and  $\Gamma_1$ ) in an applied magnetic field of  $\sim 16$  T. The experimental heat capacity of polycrystalline PrNi<sub>5</sub> was measured in 0 and 7 T magnetic fields and confirmed the presence of the anomalous behavior of the magnetic entropy, which was predicted theoretically.

## ACKNOWLEDGMENTS

The authors thank to Dr. Alexandra Pecharsky for providing the polycrystalline sample of PrNi<sub>5</sub>. The Ames Laboratory is operated by Iowa State University for the U.S. Department of Energy under Contract No. W-7405-ENG-82. This study was supported by the Office of Basic Energy Sciences, Materials Sciences Division. One of us (P.J.v.R) received financial support from the CNPq (Conselho Nacional de Desenvolvimento Científico e Tecnológico, Brazil), which is gratefully acknowledged.

\*Permanent address: Universidade do Estado do Rio de Janeiro, IF, Rua Sao Francisco Xavier Rio de Janeiro—20550-013, Brazil.

†Present address: Department of Chemistry and Biochemistry, Campus Box 215, University of Colorado, Boulder, CO 803090.

<sup>1</sup>K. Andres and S. Darack, *Physica B* **86–88**, 1071 (1997).

<sup>2</sup>G. V. Brown, *J. Appl. Phys.* **47**, 3673 (1976).

<sup>3</sup>V. K. Pecharsky and K. A. Gschneidner, Jr., *Phys. Rev. Lett.* **78**, 4494 (1997).

<sup>4</sup>K. A. Gschneidner, Jr. and V. K. Pecharsky, in *Rare Earths:*

*Science, Technology and Application III*, edited by R. C. Baudista, C. O. Bounds, T. W. Ellis, and B. T. Kilbourn (The Minerals, Metals & Materials Society, Warrendale, PA, 1997), p. 209.

<sup>5</sup>J. G. Houmann, B. D. Rainford, J. Jensen, and A. R. Mackintosh, *Phys. Rev. B* **20**, 1105 (1979).

<sup>6</sup>M. T. Hutchings, *Solid State Phys.* **16**, 227 (1964).

<sup>7</sup>N. Kaplan, D. L. Williams, and A. Graeyevski, *Phys. Rev. B* **21**, 899 (1980).

<sup>8</sup>E. Leyarovski, J. Mrachkov, A. Gilewski, and T. Mydlarz, *Phys. Rev. B* **35**, 8668 (1987).

- <sup>9</sup>A. Andreeff, V. Valter, H. Grissmann, L. P. Kaun, B. Lipold, V. Mats, and T. Franzkhaim, Joint Institute for Nuclear Research, Dubna, U.S.S.R., Commun. P14-11324, 1978 (unpublished).
- <sup>10</sup>P. A. Alekseev, A. Andreeff, H. Grissmann, L. P. Kaun, B. Lipold, W. Matz, I. P. Sadikov, O. D. Christyakov, I. A. Markova, and E. M. Savitskii, Phys. Status Solidi B **97**, 87 (1980).
- <sup>11</sup>V. M. T. S. Barthem, D. Gignoux, A. Nait-Saada, and D. Schmitt, Phys. Rev. B **37**, 1733 (1987).
- <sup>12</sup>M. Reiffers, Yu. G. Naidyuk, A. G. M. Jansen, P. Wyder, and I. K. Yanson, Phys. Rev. Lett. **62**, 1560 (1989).
- <sup>13</sup>K. W. H. Stevens, Proc. Phys. Soc. London, Sect. A **65**, 209 (1952).
- <sup>14</sup>V. K. Pecharsky, J. O. Moorman, and K. A. Gschneidner, Jr., Rev. Sci. Instrum. **68**, 4196 (1997).